Regenerative Therapy 29 (2025) 100–107

Contents lists available at ScienceDirect

Regenerative Therapy

journal homepage: http://www.elsevier.com/locate/reth

Original Article

A human iPSC-Derived myelination model for investigating fetal brain injuries

Tsuyoshi Hiraiwa [a, b], Shoko Yoshii [b, c], Jiro Kawada [d], Tohru Sugawara [b], Tomoyuki Kawasaki [b], Shinsuke Shibata [e, f], Tomoko Shindo [e], Keiya Fujimori [a], Akihiro Umezawa [b], Hidenori Akutsu [b, *]

[a] Department of Obstetrics and Gynecology, Fukushima Medical University, Fukushima, Japan
[b] Center for Regenerative Medicine, National Center for Child Health and Development, Tokyo, Japan
[c] Department of Pediatrics, Graduate School of Medicine, Chiba University, Chiba, Japan
[d] Jiksak Bioengineering, Inc., Kanagawa, Japan
[e] Electron Microscope Laboratory, Keio University School of Medicine, Tokyo, Japan
[f] Division of Microscopic Anatomy, Graduate School of Medical and Dental Sciences, Niigata University, Niigata, Japan

ARTICLE INFO

Article history:
Received 20 January 2025
Received in revised form
18 February 2025
Accepted 27 February 2025

Keywords:
Myelination
microfluidic model
Induced pluripotent stem cells
Cerebral white matter injury
Periventricular leukomalacia
Oligodendrocyte development

ABSTRACT

Cerebral white matter injuries, such as periventricular leukomalacia, are major contributors to neurodevelopmental impairments in preterm infants. Despite the clinical significance of these conditions, human-relevant models for studying fetal brain development and injury mechanisms remain limited. This study introduces a human iPSC-derived myelination model developed using a microfluidic device. The platform combines spinal cord-patterned neuronal and oligodendrocyte spheroids to recapitulate axon-glia interactions and myelination processes *in vitro*. The model successfully achieved axonal fascicle formation and compact myelin deposition, as validated by immunostaining and transmission electron microscopy. Functional calcium imaging confirmed neuronal activity within the system, underscoring its physiological relevance. While myelination efficiency was partial, with some axons remaining unmyelinated under the current conditions, this model represents a significant advancement in human myelin biology, offering a foundation for investigating fetal and perinatal brain injuries and related pathologies. Future refinements, such as improved myelination coverage and incorporating additional CNS cell types, will enhance its utility for studying disease mechanisms and enabling high-throughput drug screening.

1. Introduction

Myelination, the process of forming specialised myelin sheaths around axons, is essential for efficient signal transmission in the nervous system. This process begins in major white matter tracts and extends to intracortical fibers in the cerebral cortex, continuing through adolescence and into early adulthood. Impaired myelination disrupts neural circuit formation and has been implicated in a range of neurodevelopmental and neurodegenerative disorders. The orchestration of myelination depends on oligodendrocyte differentiation and precise alignment along axons, emphasising the importance of studying axon-glia interactions using human-specific models.

Premature birth and its associated complications are major contributors to cerebral white matter injuries, including impaired myelination, which significantly affect long-term neurodevelopmental outcomes. Advances in neuroimaging techniques, such as MRI, have revealed characteristic reductions in premyelinating oligodendrocytes [1,2]; however, detecting myelination failure at term-equivalent age remains challenging due to the limited white matter volume (~5 %) in the developing brain [3,4]. Moreover, current experimental models, including rodent models and two-dimensional cell cultures, fall short in replicating the complexity of human neuronal tissue development. While valuable for studying general neurodevelopment, Rodent models differ

* Corresponding author. Department of Reproductive Medicine, Center for Regenerative Medicine, National Center for Child Health and Development (NCCHD), Okura 2-10-1, Setagaya-ku, Tokyo 157-8535, Japan.
E-mail address: akutsu-h@ncchd.go.jp (H. Akutsu).

Peer review under responsibility of the Japanese Society for Regenerative Medicine.

https://doi.org/10.1016/j.reth.2025.02.014

significantly in the timing and organization of myelination processes compared to humans. Similarly, two-dimensional cell cultures lack the three-dimensional architecture necessary to recapitulate axon-glia interactions and the spatial organization of white matter. These limitations hinder progress in understanding axonal and glial responses to injury in a human-relevant context [5–7].

Human pluripotent stem cells (PSCs) offer unprecedented opportunities to model human nervous system development and investigate the cellular mechanisms underlying neurological disorders. While cerebral organoids and microdevice technologies have enabled the *in vitro* replication of axonal structures [8–11], existing models struggle to recreate the myelination process effectively. This gap presents a critical barrier to understanding the nuances of axon-glia interactions in health and disease. Specifically, questions regarding the timing and molecular cues for oligodendrocyte differentiation, the mechanisms guiding their precise alignment along axons, and the influence of neuronal activity on myelin maturation remain unresolved. Advanced systems capable of addressing these aspects are urgently needed to capture better the complexity of human myelin formation and its pathological disruptions [12,13].

In this study, we present a novel microfluidic platform that models myelination by integrating human induced pluripotent stem cell (iPSC)-derived neuronal and oligodendrocyte spheroids within a compartmentalized system. The resulting axonal fascicles, wrapped by oligodendrocytes, recapitulate key aspects of human myelin biology. This advanced model provides a robust platform for studying axon-glia interactions, human brain development, and disorders related to myelination, addressing critical gaps in the understanding of fetal and perinatal brain injuries.

2. Materials and methods

2.1. Human iPSCs

The Edom-human iPSC line, previously established in our laboratory using the CytoTune™-iPS Sendai Reprogramming Kit (Thermo Fisher Scientific, Waltham, MA), was used in this study [14]. Cells were cultured in StemFlex™ Medium (Thermo Fisher Scientific) on vitronectin-coated plates and maintained at 37 °C under a humidified atmosphere with 5 % CO_2 [15]. For differentiation into neurons and oligodendrocytes, an enhanced green fluorescent protein (EGFP)-Edom-iPSC line was utilised [16]. This line constitutively expresses EGFP under a cytomegalovirus promoter, facilitated by a hyperactive PiggyBac vector [17], allowing visualisation of cell development.

The culture medium was replaced every other day, except on the day following passaging. Cells were passaged approximately once per week using Accutase (Thermo Fisher Scientific).

2.2. Cerebral and oligodendroglial spheroid generation

2.2.1. Neural induction and cryopreservation

Neuronal differentiation was conducted based on a previously established protocol with modifications [18]. Human iPSCs cultured under feeder-free conditions were seeded into six-well plates at a density of $2–2.5 \times 10^4$ cells/cm^2. Approximately 24 h after seeding, the culture medium was replaced with Gibco PSC Neural Induction Medium (Thermo Fisher Scientific), comprising Neurobasal medium and Gibco PSC Neural Induction Supplement. The medium was changed every other day until Day 4, after which it was replaced daily as the cells approached confluence.

On Day 8 of neural induction, primitive neural stem cells (NSCs) were dissociated using Accutase (Thermo Fisher Scientific) and replated onto Geltrex-coated dishes at a density of $0.5–1 \times 10^5$ cells/cm^2 in NSC expansion medium. The NSC expansion medium consisted of 50 % Neurobasal medium, 50 % Advanced Dulbecco's Modified Eagle's Medium: Nutrient Mixture F-12 (DMEM/F12) (Thermo Fisher Scientific), and neural induction supplement. The medium was changed every other day, and NSCs reached confluence by Day 5 after plating.

Primitive NSCs were then dissociated and cryopreserved in NSC expansion medium supplemented with 20 % dimethyl sulfoxide (DMSO) (Sigma-Aldrich, St. Louis, MI).

2.2.2. Neural spheroid generation

Cryopreserved primitive NSCs were used for neural spheroid generation. Thawed NSCs were plated onto Geltrex-coated six-well plates in NSC expansion medium, with the medium refreshed every other day until the cells reached confluence. Neural spheroids were subsequently generated following a previously described protocol [8,19], with modifications.

Confluent primitive NSCs were dissociated using Accutase and seeded at a density of 1×10^4 cells per well in low-adhesion V-bottom 96-well plates (Sumitomo Bakelite, Tokyo, Japan). The cells were cultured in neural spheroid medium, which comprised 47 % Neurobasal medium, 47 % Advanced DMEM/F12, 1 % N2 supplement, 2 % B27 supplement, 1 % Penicillin/Streptomycin, 1 % GlutaMax, 1 % nonessential amino acids, and 25 μM β-mercaptoethanol (all from Thermo Fisher Scientific).

2.3. Oligodendrocyte spheroid generation

Oligodendrocyte differentiation was performed following previously established protocols with modifications [20,21]. Human iPSCs were dissociated using Accutase and plated into six-well plates in StemFlex™ medium. Once the cells reached approximately 20 % confluence, the medium was replaced on Day 0 with Neural Induction Medium supplemented with 100 nM Retinoic Acid (RA; Sigma-Aldrich), 10 μM SB431542 (a BMP signaling inhibitor; Tocris Bioscience, Bristol, UK), and 100 nM LDN193189 (a TGF-beta signaling inhibitor; Tocris Bioscience). The medium was changed daily until Day 7.

On Day 8, the Neural Induction Medium was replaced with N2 medium (1 % N2 supplement in basal medium) supplemented with 100 nM RA and 1 μM Smoothened Agonist (SAG; Millipore, Burlington, MA). Cells were cultured under these conditions for an additional three days. On Day 12, the cells were dissociated using Accutase and seeded at a density of 1×10^4 cells per well in low-adhesion V-bottom 96-well plates. The cells were maintained in N2B27 medium supplemented with 100 nM RA and 1 μM SAG to promote spheroid formation.

2.4. Coculture of neuronal and oligodendrocyte spheroids in microfluidic device

The nerve organoid microfluidic device (Cat. JKSK_S0001U, Jiksak Bioengineering, Kanagawa, Japan) (Fig. 1; see also Kawada et al. [10]) was pre-coated with Matrigel (Corning, Corning, NY) to enhance cell attachment and axon alignment. On Day 20, neuronal spheroids were introduced into the microfluidic device and cultured in neuronal spheroid medium (N2B27 medium) supplemented with 20 ng/mL brain-derived neurotrophic factor (BDNF; Thermo Fisher Scientific). The medium was replaced every three days. Axon fascicles began to form within the microchannel approximately 15 days after neuronal spheroids were introduced into the device.

In parallel, Day 20 oligodendrocyte spheroids were transferred into separate microfluidic devices and maintained in platelet

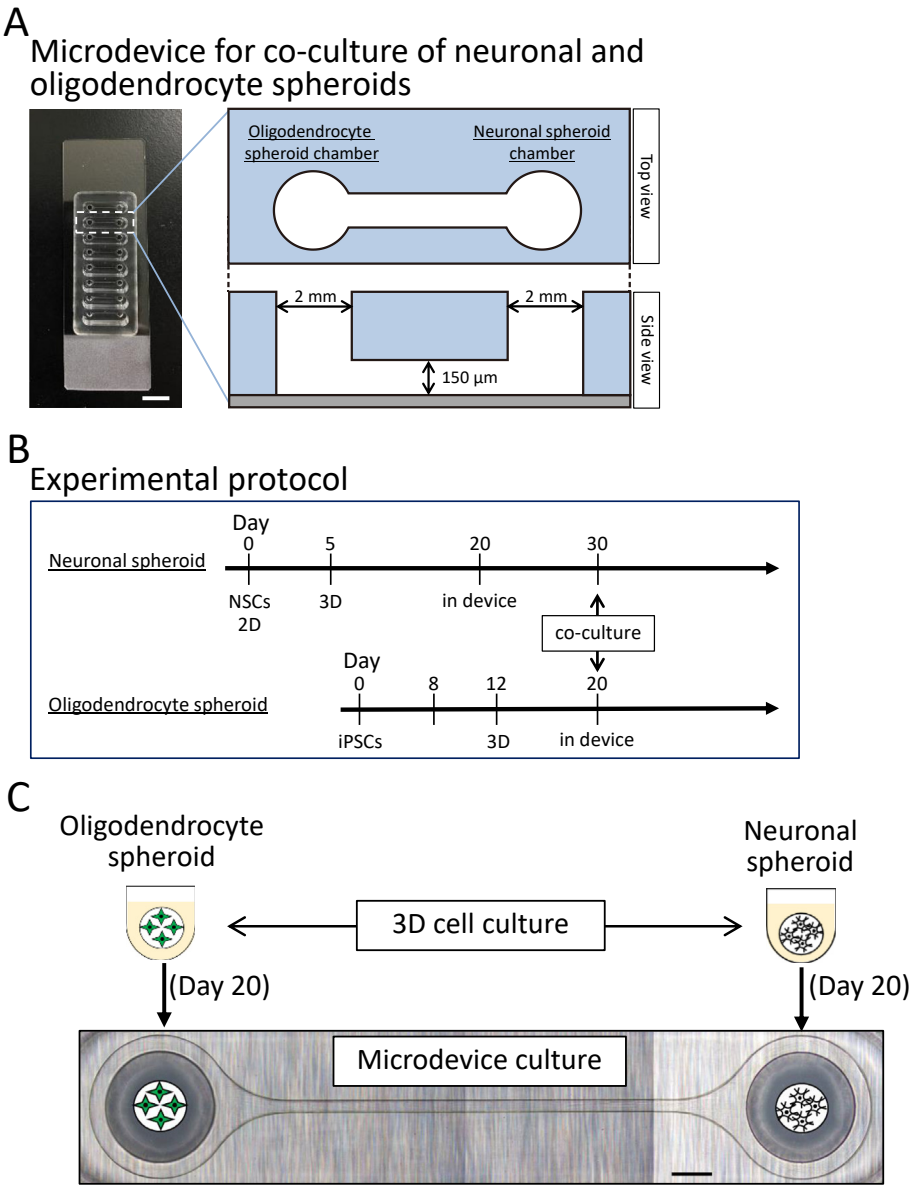

Fig. 1. Microfluidic Co-Culture System for Axon-Oligodendrocyte Interactions. (A) Photograph of the microfluidic device used for the co-culture system, showing distinct chambers for neuronal and oligodendrocyte spheroids connected by microchannels to enable axon-oligodendrocyte interactions. A schematic illustration of the device design is provided: the top view (upper panel) displays the layout of the chambers and connecting microchannels, while the side view (lower panel) highlights the chamber dimensions and microchannel architecture. Scale bar: 5 mm. (B) Workflow of the co-culture system in the microfluidic device. Neuronal and oligodendrocyte spheroids were matured separately in their respective chambers before co-culture, facilitating axon extension and interaction with oligodendrocytes. (C) Bright-field image showing the microfluidic device after neuronal and oligodendrocyte spheroids were introduced. Axons extend from the neuronal spheroids through the microchannels toward the oligodendrocyte chamber. Scale bar: 500 μm.

derived growth factor (PDGF) medium. This medium consisted of basal medium supplemented with 1 % N2 supplement, 2 % B27 supplement, 25 μg/mL insulin, 10 ng/mL platelet-derived growth factor-AA (PDGF-AA; Sigma-Aldrich), 10 ng/mL insulin-like growth factor-1 (IGF-1; Thermo Fisher Scientific), 5 ng/mL hepatocyte growth factor (HGF; Fujifilm-Wako, Tokyo, Japan), 10 ng/mL neurotrophin-3 (NT-3; Thermo Fisher Scientific), 100 ng/mL biotin (Sigma-Aldrich), 1 μM N6,2-*O*-dibutyryladenosine 3′,5′-cyclic monophosphate sodium salt (cAMP; Sigma-Aldrich), and 60 ng/mL 3,3′,5-triiodo-L-thyronine (T3; Sigma-Aldrich). Half of the medium was replaced every three days throughout the culture period. By 20–30 days after introducing the oligodendrocyte spheroids, differentiating oligodendrocytes extended processes along the axon fascicles formed by the neuronal spheroids. This alignment and interaction between neuronal and oligodendrocyte spheroids within the microfluidic system demonstrated functional coculture of axon-glia interactions in a controlled three-dimensional environment.

2.5. Immunofluorescence staining

Organoid tissues were fixed in 4 % paraformaldehyde for 20 min at 4 °C and permeabilized with 0.1 % Triton X-100 (Sigma-Aldrich) for 10 min at room temperature. Organoids extracted from the microfluidic device were directly subjected to immunostaining. After blocking with 5 % normal goat serum in Dulbecco's phosphate-buffered saline (DPBS; Thermo Fisher Scientific) for 30 min at room temperature, the samples were incubated overnight at 4 °C with primary antibodies. Following DPBS washes, secondary antibodies conjugated to Alexa Fluor 488 or Alexa Fluor

546 (Thermo Fisher Scientific) were applied for 30 min at room temperature. After final DPBS washes, samples were mounted using DAPI-containing mounting medium.

The primary antibodies used were: Anti-TAU1 (MAB3420, Merck Millipore, Billerica, MA, USA; 1:1000), anti-myelin basic protein (MBP; bs-0380R, Bioss, Woburn, MA, USA; 1:100), anti-Olig2 (NBP1-28667, Novus Biologicals, Centennial, CO, USA; 1:1000), and anti-O4 (MAB1326, R&D Systems, Minneapolis, MN, USA; 1:40). Fluorescence images were acquired using a BZ-X700 fluorescence microscope (Keyence, Osaka, Japan).

2.6. Electron microscope (EM) analysis

Electron microscopy analysis followed a previously described protocol [22] with the following modifications. Organoid samples were fixed in 2.5 % glutaraldehyde in 0.1 M phosphate buffer (Muto Pure Chemicals, Tokyo, Japan) and post-fixed with 1.0 % osmium tetroxide (TAAB Laboratories, England, UK). Samples were subjected to a series of dehydration steps with ethanol and n-butyl glycidyl ether (QY1, Okenshoji Co. Ltd., Tokyo, Japan). Ultrathin sections from epoxy resin-embedded blocks were mounted on copper grids and examined using a transmission electron microscope (JEM-1400Plus, JEOL, Tokyo, Japan) operated at 100 kV to obtain ultrahigh-resolution images. Whole-section imaging was conducted using a multibeam scanning electron microscope (mSEM; MultiSEM 505, Carl Zeiss).

2.7. Calcium imaging

Calcium imaging was conducted using the calcium indicator dye Fluo-4 AM (Dojindo, Tokyo, Japan), prepared and applied according to the manufacturer's instructions. After extraction from the microfluidic culture device, the tissue was incubated in a loading buffer containing 140 mM NaCl, 5 mM KCl, 2.5 mM $CaCl_2$, 1 mM $MgCl_2$, 10 mM HEPES and 10 mM glucose (pH 7.0) for 30 min. Following a DPBS wash, the tissue was transferred to BrainPhys™ Neuronal medium (StemCell Technologies, Vancouver, Canada) supplemented with N2 and B27 supplements.

A neuronal spheroid was positioned between two tungsten probe needles (SW6-1, Omniphysics, Kanagawa, Japan) for imaging. Fluorescence intensity changes were recorded using an inverted fluorescence microscope (Keyence) during electrical stimulation. Electrical stimulation was applied via a microcontroller (AVR, Microchip Technology Japan, Tokyo, Japan) using a single positive square pulse (1 ms duration) at 4 V, with a 10-s interval between stimulations. Experiments were performed at room temperature.

3. Results

3.1. Development of a compartmentalized nerve organoid for studying axon-glia interactions

To mimic the developing cerebral tract, a nerve organoid microfluidic device (Jiksak Bioengineering) was used to co-culture human iPSC-derived neuronal and oligodendrocyte spheroids. The device features distinct chambers connected by microchannels (Fig. 1A), enabling spatial segregation of neuronal cell bodies and axonal projections, thus facilitating controlled axon-glia interactions. Neurons extended axons naturally, guided by intrinsic growth and fasciculation mechanisms, with minimal external manipulation [10].

Human iPSCs were differentiated into NSCs and cultured as spheroids in low-adhesion plates for 15 days (Fig. 1B and C). At Day 20, NSC spheroids were transferred into the microfluidic device to induce axon fascicle formation. The device included a chamber for spheroid placement, microchannels to guide axon fascicle extension, and a target chamber for axon terminals (Fig. 1C). GFP-labelled human iPSC-derived neurons spontaneously extended axons from the spheroids into the microchannels, with progressive axonal extension observed at 5-, 10-, and 15-days post-transfer. This process resulted in the formation of organized fascicles as subsequent axons followed the initial growth (Fig. 2A1).

Concurrently, oligodendrocyte precursor cells (OPCs) migrated from oligodendrocyte spheroids into the microchannels, aligning themselves along the axons (Fig. 2A2). Over time, OPCs matured and began interacting with the axonal bundles, reflecting the dynamic myelination process. By Day 30, the system exhibited robust compartmentalization, with well-aligned axonal tracts connecting the two chambers (Fig. 2B and C).

This nerve organoid model successfully recapitulates critical aspects of axon-glia interactions, including axonal alignment and the initiation of myelination. It establishes a promising platform for investigating neural development and pathologies associated with myelin.

3.2. Comprehensive validation of axonal and myelin structures within a microfluidic myelination model

The engineered axonal fascicles formed in the microfluidic system demonstrated structural organization and robustness (Figs. 2B and 3A). These fascicles were continuous, unidirectional, and consistently aligned within the microchannels. Immunostaining confirmed their axonal identity, showing uniform TAU1 expression along the entire bundle (Fig. 3B). This accurately replicates physiological axonal architecture, offering a well-controlled platform for studying axon-glia interactions and the mechanisms underlying human myelination.

To evaluate neuronal activity within the axonal fascicles, calcium imaging with Fluo-4 AM dye was performed (Movie S1). Electrical stimulation elicited synchronized fluorescence signals, indicating robust neuronal activation along the fascicles. This functional connectivity and excitability validate the system's potential for investigating dynamic neural activity and axon-glia interactions in a human-specific context.

Supplementary video related to this article can be found at https://doi.org/10.1016/j.reth.2025.02.014

The differentiation and maturation of oligodendrocytes were monitored throughout the culture process. At Day 12, prior to their integration into the microfluidic device, oligodendrocytes exhibited uniform expression of OLIG2, confirming their identity as OPCs (Fig. 3C). Following 30 days of co-culture within the device, extensive expression of O4, a marker of mature oligodendrocytes, was observed (Fig. 3C). This progression from progenitor to mature oligodendrocyte phenotype highlights successful differentiation and integration within the microfluidic environment.

Immunostaining for MBP revealed extensive myelination along the axonal fascicles, indicative of active oligodendrocyte-axon interactions in the three-dimensional culture (Fig. 3D). Transmission electron microscopy analysis further validated the presence of compact myelin, characterized by electron-dense, concentrically wrapped membrane lamellae (Fig. 3E, Fig. S1). These findings confirm that the model successfully replicates the structural and molecular features of CNS myelination.

This advanced *in vitro* system provides a robust platform for mechanistic investigations of axon-oligodendrocyte interactions, neural network development, and myelin biology. It holds significant potential for studying myelin-related disorders and advancing therapeutic strategies.

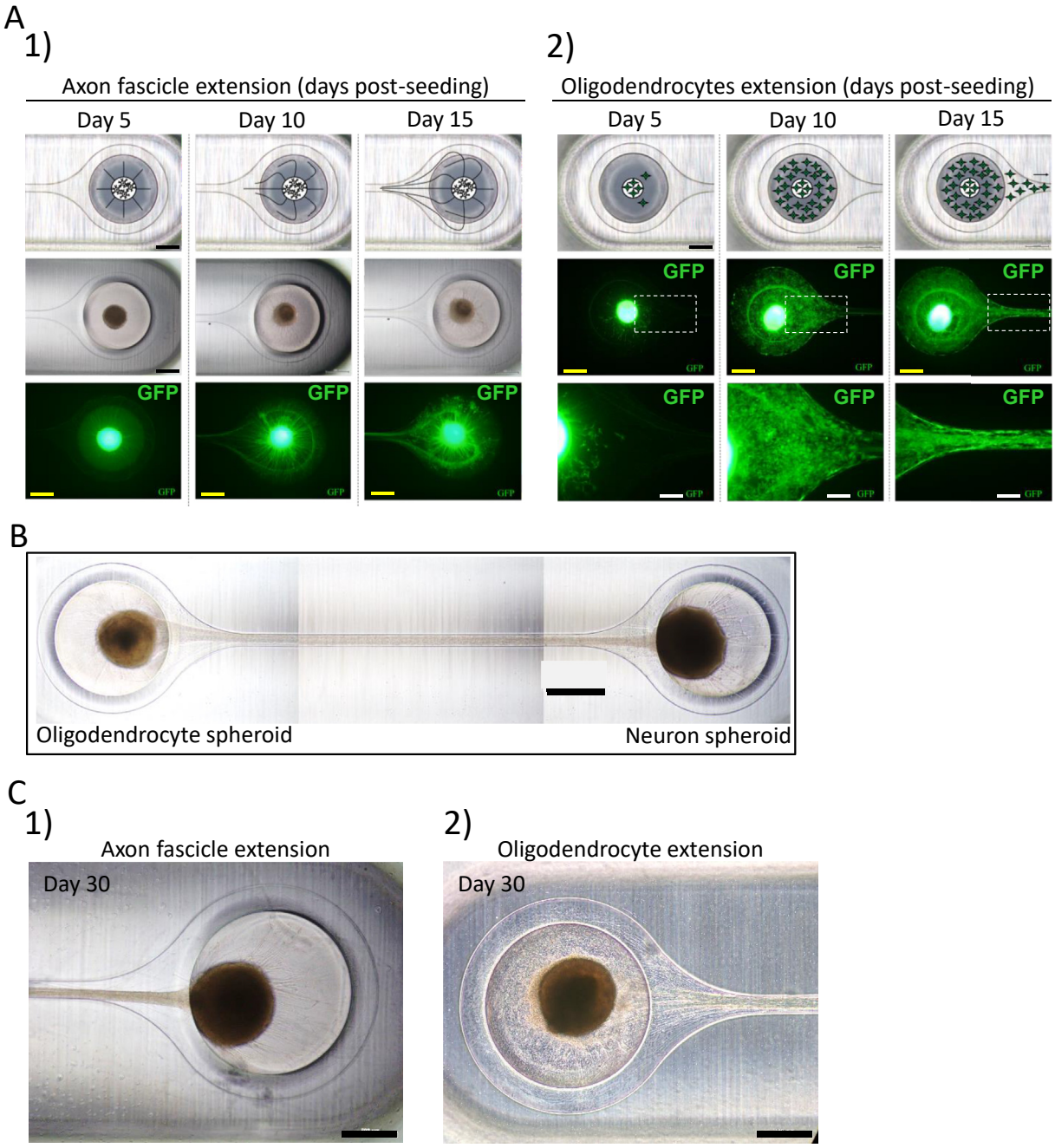

Fig. 2. Axonal and Oligodendrocyte Extensions Within the Microfluidic Co-Culture System. (A) Sequential bright-field and fluorescence images showing axonal and oligodendrocyte outgrowth within the microfluidic device. (1) The top and middle rows depict bright-field images of axonal extensions from neuronal spheroids, forming organized fascicles within the microchannels. Scale bar: 500 μm (black). The bottom row highlights GFP-positive axonal projections from Edom-iPSC-derived neuronal spheroids, showing progressive alignment and bundling. Scale bar: 500 μm (yellow). (2) Bright-field (top row) and fluorescence (middle and bottom rows) images of oligodendrocyte extensions. The bright-field images show spheroid morphology and cellular projections (top row). The middle row presents GFP-positive oligodendrocyte processes extending through the microchannels, with regions outlined by dashed boxes shown at higher magnification in the bottom row, demonstrating clear extension and alignment. Scale bars: 500 μm (black and yellow) and 200 μm (white). (B) Bright-field image of the co-culture system after 30 days, showing axonal extensions from the neuronal spheroid (left) and cellular projections from the oligodendrocyte spheroid (right), converging within the microchannel. Scale bar: 1 mm. (C) High-magnification bright-field images of the neuronal and oligodendrocyte spheroids in the microfluidic device after 30 days of culture. (1) Neuronal spheroid showing robust axonal alignment and growth into the microchannel. (2) Oligodendrocyte spheroid with cellular projections extending into the microchannel. Scale bars: 500 μm.

4. Discussion

In this study, we established a human iPSC-derived myelination model using a microfluidic device, demonstrating its capacity to replicate key features of axon-glia interactions and myelin formation *in vitro*. This model addresses the need for human-relevant experimental systems to investigate fetal brain maturation, perinatal brain injury, and related neurological disorders, such as cerebral palsy, hypoxic-ischemic encephalopathy, multiple sclerosis, and leukodystrophies. Existing models often lack the complexity and specificity of human neural development, limiting their utility in understanding disease mechanisms and developing therapeutic

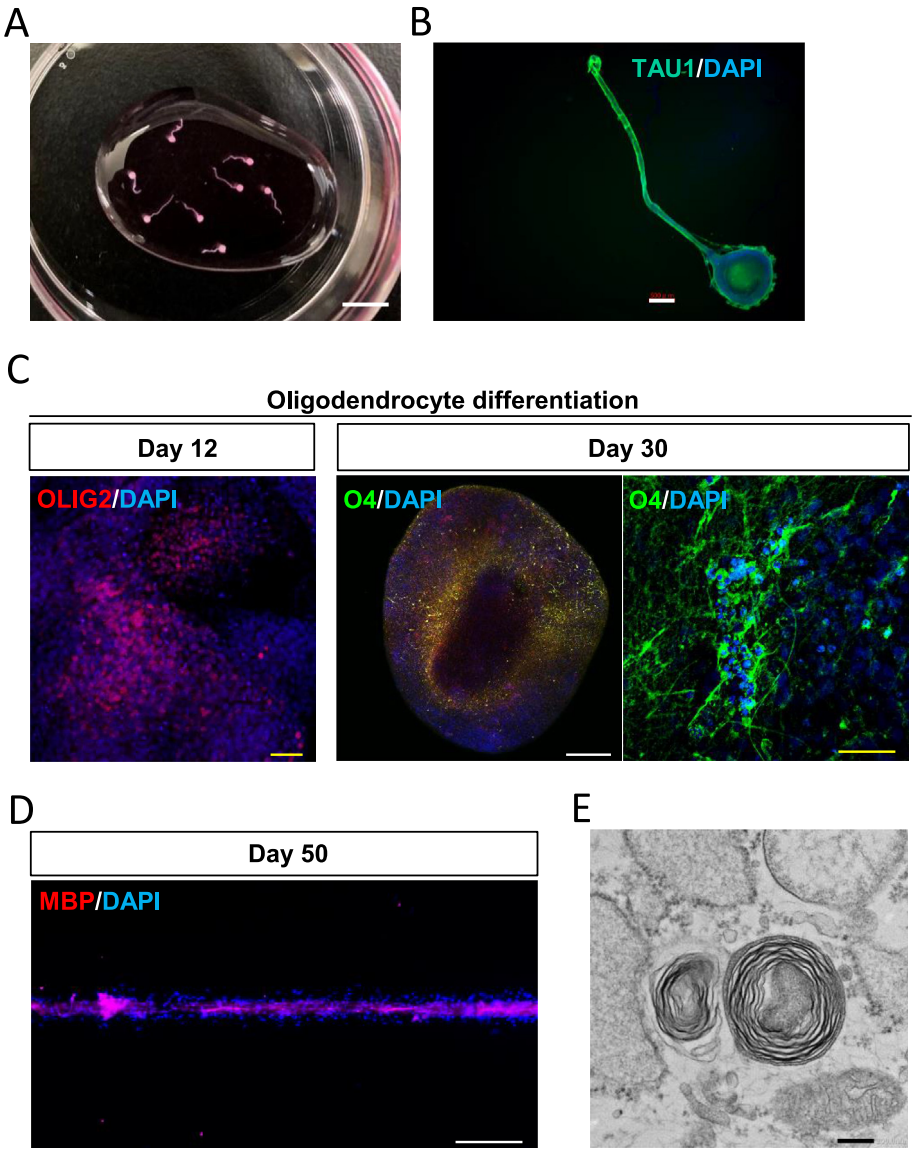

Fig. 3. Comprehensive Characterization of Neuronal and Oligodendrocyte Differentiation, Interaction, and Myelination in a Co-Culture System. (A) Representative image of a neuronal organoid extracted from the microfluidic device after 60 days of culture, displaying robust structural integrity and maintaining its shape and organization. Scale bar: 5 mm. (B) Immunofluorescence image of the neuronal organoid stained with the axon-specific marker TAU1 (green) and counterstained with DAPI (blue) for nuclei. Uniform TAU1-positive staining confirms the axonal identity of the neuronal structures. Scale bar: 500 μm. (C) Validation of oligodendrocyte differentiation via immunofluorescence staining. (1) At Day 12 of differentiation, before spheroid formation, OLIG2-positive staining (red) confirms the identity of oligodendrocyte progenitor cells. (2) At Day 30, a low-magnification image of the spheroid within the microfluidic device shows widespread O4-positive staining (green), indicating pre-myelinating oligodendrocytes. (3) High-magnification view of the Day 30 spheroid demonstrates extensive O4-positive staining (green), with well-developed oligodendrocyte processes. DAPI (blue) highlights nuclei. Scale bars: 50 μm (yellow) and 200 μm (white). (D) Immunofluorescence image of the co-culture system at Day 50, showing MBP-positive (red) staining along axonal structures, confirming interactions between myelinating oligodendrocytes and axons within the microfluidic device. DAPI (blue) was used for nuclear counterstaining. Scale bar: 500 μm. (E) Transmission electron microscopy (TEM) image of co-cultured neuronal and oligodendrocyte tissue showing compact myelin sheaths formed around axons. The characteristic multilayered myelin lamellae concentrically wrapped around axons are clearly visible, indicating successful myelination. Scale bar: 200 nm.

strategies [23–25]. By integrating compartmentalized neuronal and oligodendrocyte spheroids within a microfluidic device, our platform fills this gap and offers a more physiologically relevant environment than conventional two-dimensional co-cultures [19,26]. Notably, the model facilitates the directed alignment of axons and oligodendrocytes, enabling compact myelin formation in a significantly shorter culture period compared to organoid-based or animal-derived models [27,28]. Additionally, the microfluidic design permits precise control over the local microenvironment, including gradient delivery of growth factors, which is often challenging in traditional systems [29,30]. Collectively, these features enhance the model's physiological relevance and scalability, making it well-suited for examining human-specific axon-glia interactions and myelin-related pathologies.

This configuration enables the directed alignment of axons and oligodendrocytes, facilitating compact myelin formation within a significantly shorter culture period compared to existing organoid-based or animal-derived models [27,28]. Furthermore, the microfluidic design allows for precise control of the microenvironment, including the gradient delivery of growth factors, which is challenging to achieve in traditional systems [29,30]. These features collectively enhance the physiological relevance and scalability of the model, positioning it as a valuable tool for investigating human-specific axon-glia interactions and myelin-related pathologies.

Our results indicate that this microfluidic model supports early and robust myelination in alignment with the developmental timeline of the spinal cord, thereby reducing the overall culture duration. Although this efficiency is advantageous, myelination was observed in only a subset of axons, highlighting the need for further optimization to achieve more uniform coverage [27]. Incorporating region-specific patterning could broaden the model's utility, particularly in regenerative medicine and drug discovery.

While we did not quantify the purity of neuronal and oligodendrocyte populations, our differentiation protocols consistently yield robust spheroids. Neuronal spheroids efficiently form axonal fascicles, while oligodendrocyte spheroids reliably support myelination. However, oligodendrocyte differentiation requires a longer induction period, which may impact myelination efficiency. Optimizing this process could further enhance myelination coverage and reproducibility.

Our model also holds potential for studying adult-onset neurological diseases, such as multiple sclerosis and age-related white matter degeneration. To extend its applicability to these conditions, modifications such as incorporating aging-related cellular changes, integrating neuroinflammatory components like microglia, and extending the culture duration would be necessary. These refinements could enable the study of chronic demyelination and repair mechanisms in a human-relevant system.

Several limitations should be addressed to improve physiological relevance. The absence of microglia, essential for myelin maintenance, immune responses, and regulation of neuronal activity, represents a critical gap. Integrating microglia and other CNS cell types (e.g., astrocytes) could provide a more comprehensive environment by introducing neuroinflammation, injury repair, and cellular crosstalk during myelination. For instance, microglia promote oligodendrocytes through cytokine secretion and clearance of myelin debris, while astrocytes support axon-glia signaling and regulate extracellular ion balance [31–33]. Integrating these cells may enhance myelination efficiency and facilitate repair following injury. Additionally, scaling the system for high-throughput analysis with fluorescent myelin-specific markers could streamline drug screening and disease modeling [34–36].

In summary, our microfluidic myelination model represents a significant step forward in studying axon-glia interactions and human myelin biology. Its relevance is particularly evident in fetal and perinatal brain injuries, as this model uniquely replicates human-specific myelin formation in a three-dimensional environment. These attributes have relevance for investigating fetal and perinatal brain injuries, as well as demyelinating disorders. Although improvements in myelination efficiency, cellular diversity, and scalability remain necessary, this model provides a strong foundation for future studies. With continued development, it promises to clarify the underlying mechanisms of neurodevelopmental and demyelinating conditions, thereby contributing to more effective therapeutic approaches.

Declaration of competing interest

The authors have no conflict of interest to report.

Acknowledgments

We are grateful to the members of our laboratory for their helpful discussions. This work was supported by JSPS Grant-in-Aid for Scientific Research (A) to HA (JP20H00550); the National Center for Child Health and Development (2022A-2) to HA. The funders had no role in the study design, data collection and analysis, decision to publish, nor the preparation of the manuscript.

Appendix A. Supplementary data

Supplementary data to this article can be found online at https://doi.org/10.1016/j.reth.2025.02.014.

References

[1] Back SA. White matter injury in the preterm infant: pathology and mechanisms. Acta Neuropathol 2017 Sep;134(3):331–49. https://doi.org/10.1007/s00401-017-1718-6.
[2] Deng W. Neurobiology of injury to the developing brain. Nat Rev Neurol 2010 Jun;6(6):328–36. https://doi.org/10.1038/nrneurol.2010.53.
[3] Hüppi PS, Warfield S, Kikinis R, Barnes PD, Zientara GP, Jolesz FA, et al. Quantitative magnetic resonance imaging of brain development in premature and mature newborns. Ann Neurol 1998 Feb;43(2):224–35. https://doi.org/10.1002/ana.410430213.
[4] Tau GZ, Peterson BS. Normal development of brain circuits. Neuropsychopharmacology 2010 Jan;35(1):147–68. https://doi.org/10.1038/npp.2009.115.
[5] Volpe JJ. Brain injury in premature infants: a complex amalgam of destructive and developmental disturbances. Lancet Neurol 2009 Jan;8(1):110–24. https://doi.org/10.1016/S1474-4422(08)70294-1.
[6] Yang Z, Covey MV, Bitel CL, Ni L, Jonakait GM, Levison SW. Sustained neocortical neurogenesis after neonatal hypoxic/ischemic injury. Ann Neurol 2007 Mar;61(3):199–208. https://doi.org/10.1002/ana.21068.
[7] Sizonenko SV, Camm EJ, Dayer A, Kiss JZ. Glial responses to neonatal hypoxic-ischemic injury in the rat cerebral cortex. Int J Dev Neurosci 2008 Feb;26(1):37–45. https://doi.org/10.1016/j.ijdevneu.2007.08.014.
[8] Lancaster MA, Knoblich JA. Generation of cerebral organoids from human pluripotent stem cells. Nat Protoc 2014 Oct;9(10):2329–40. https://doi.org/10.1038/nprot.2014.158.
[9] Giandomenico SL, Sutcliffe M, Lancaster MA. Generation and long-term culture of advanced cerebral organoids for studying later stages of neural development. Nat Protoc 2021 Feb;16(2):579–602. https://doi.org/10.1038/s41596-020-00433-w.
[10] Kawada J, Kaneda S, Kirihara T, Maroof A, Levi T, Eggan K, et al. Generation of a motor nerve organoid with human stem cell-derived neurons. Stem Cell Rep 2017 Nov 14;9(5):1441–9. https://doi.org/10.1016/j.stemcr.2017.09.021.
[11] Shao Y, Fu J. Engineering multiscale structural orders for high-fidelity embryoids and organoids. Cell Stem Cell 2022 May 5;29(5):722–43. https://doi.org/10.1016/j.stem.2022.04.003.
[12] Marangon D, Caporale N, Boccazzi M, Abbracchio MP, Testa G, Lecca D. Novel in vitro experimental approaches to study myelination and remyelination in the central nervous system. Front Cell Neurosci 2021 Oct 14;15:748849. https://doi.org/10.3389/fncel.2021.748849.
[13] Yu Q, Guan T, Guo Y, Kong J. The initial myelination in the central nervous system. ASN Neuro 2023 Jan-Dec;15:17590914231163039. https://doi.org/10.1177/17590914231163039.
[14] Nishino K, Toyoda M, Yamazaki-Inoue M, Fukawatase Y, Chikazawa E, Sakaguchi H, et al. DNA methylation dynamics in human induced pluripotent stem cells over time. PLoS Genet 2011 May;7(5):e1002085. https://doi.org/10.1371/journal.pgen.1002085.
[15] Isono W, Kawasaki T, Ichida JK, Ayabe T, Hiraike O, Umezawa A, et al. The combination of dibenzazepine and a DOT1L inhibitor enables a stable maintenance of human naïve-state pluripotency in non-hypoxic conditions. Regen Ther 2020 Sep 2;15:161–8. https://doi.org/10.1016/j.reth.2020.08.001.
[16] Tsuruta S, Kawasaki T, Machida M, Iwatsuki K, Inaba A, Shibata S, et al. Development of human gut organoids with resident tissue macrophages as a model of intestinal immune responses. Cell Mol Gastroenterol Hepatol 2022;14(3):726–729.e5. https://doi.org/10.1016/j.jcmgh.2022.06.006.
[17] Yamada M, Sugawara T, Usami S, Nakanishi R, Akustu H. Using piggyBac transposon gene expression vectors to transfect Zscan5b gene into mouse pluripotent stem cells. STAR Protoc 2021 Sep 11;2(3):100811. https://doi.org/10.1016/j.xpro.2021.100811.
[18] Yan Y, Shin S, Jha BS, Liu Q, Sheng J, Li F, et al. Efficient and rapid derivation of primitive neural stem cells and generation of brain subtype neurons from human pluripotent stem cells. Stem Cells Transl Med 2013 Nov;2(11):862–70. https://doi.org/10.5966/sctm.2013-0080.
[19] Lancaster MA, Renner M, Martin CA, Wenzel D, Bicknell LS, Hurles ME, et al. Cerebral organoids model human brain development and microcephaly. Nature 2013 Sep 19;501(7467):373–9. https://doi.org/10.1038/nature12517.
[20] Douvaras P, Wang J, Zimmer M, Hanchuk S, O'Bara MA, Sadiq S, et al. Efficient generation of myelinating oligodendrocytes from primary progressive multiple sclerosis patients by induced pluripotent stem cells. Stem Cell Rep 2014 Aug 12;3(2):250–9. https://doi.org/10.1016/j.stemcr.2014.06.012.
[21] Douvaras P, Fossati V. Generation and isolation of oligodendrocyte progenitor cells from human pluripotent stem cells. Nat Protoc 2015 Aug;10(8):1143–54. https://doi.org/10.1038/nprot.2015.075.
[22] Shibata S, Iseda T, Mitsuhashi T, Oka A, Shindo T, Moritoki N, et al. Large-area fluorescence and electron microscopic correlative imaging with multibeam scanning electron microscopy. Front Neural Circ 2019 May 8;13:29. https://doi.org/10.3389/fncir.2019.00029.

[23] Semple BD, Blomgren K, Gimlin K, Ferriero DM, Noble-Haeusslein LJ. Brain development in rodents and humans: identifying benchmarks of maturation and vulnerability to injury across species. Prog Neurobiol 2013 Jul-Aug;106–107:1–16. https://doi.org/10.1016/j.pneurobio.2013.04.001.
[24] Zeiss CJ. Comparative milestones in rodent and human postnatal central nervous system development. Toxicol Pathol 2021 Dec;49(8):1368–73. https://doi.org/10.1177/01926233211046933.
[25] Gargareta VI, Reuschenbach J, Siems SB, Sun T, Piepkorn L, Mangana C, et al. Conservation and divergence of myelin proteome and oligodendrocyte transcriptome profiles between humans and mice. Elife 2022 May 11;11:e77019. https://doi.org/10.7554/eLife.77019.
[26] Danjo T, Eiraku M, Muguruma K, Watanabe K, Kawada M, Yanagawa Y, et al. Subregional specification of embryonic stem cell-derived ventral telencephalic tissues by timed and combinatory treatment with extrinsic signals. J Neurosci 2011 Feb 2;31(5):1919–33. https://doi.org/10.1523/JNEUROSCI.5128-10.2011.
[27] Madhavan M, Nevin ZS, Shick HE, Garrison E, Clarkson-Paredes C, Karl M, et al. Induction of myelinating oligodendrocytes in human cortical spheroids. Nat Methods 2018 Sep;15(9):700–6. https://doi.org/10.1038/s41592-018-0081-4.
[28] Kim H, Xu R, Padmashri R, Dunaevsky A, Liu Y, Dreyfus CF, et al. Pluripotent stem cell-derived cerebral organoids reveal human oligodendrogenesis with dorsal and ventral origins. Stem Cell Rep 2019 May 14;12(5):890–905. https://doi.org/10.1016/j.stemcr.2019.04.011.
[29] Shin Y, Han S, Jeon JS, Yamamoto K, Zervantonakis IK, Sudo R, et al. Microfluidic assay for simultaneous culture of multiple cell types on surfaces or within hydrogels. Nat Protoc 2012 Jun 7;7(7):1247–59. https://doi.org/10.1038/nprot.2012.051.
[30] Choi YJ, Park J, Lee SH. Size-controllable networked neurospheres as a 3D neuronal tissue model for Alzheimer's disease studies. Biomaterials 2013 Apr;34(12):2938–46. https://doi.org/10.1016/j.biomaterials.2013.01.038.
[31] Kalafatakis I, Karagogeos D. Oligodendrocytes and microglia: key players in myelin development, damage and repair. Biomolecules 2021 Jul 20;11(7):1058. https://doi.org/10.3390/biom11071058.
[32] Peferoen L, Kipp M, van der Valk P, van Noort JM, Amor S. Oligodendrocyte-microglia cross-talk in the central nervous system. Immunology 2014 Mar;141(3):302–13. https://doi.org/10.1111/imm.12163.
[33] Molina-Gonzalez I, Holloway RK, Jiwaji Z, Dando O, Kent SA, Emelianova K, et al. Astrocyte-oligodendrocyte interaction regulates central nervous system regeneration. Nat Commun 2023 Jun 8;14(1):3372. https://doi.org/10.1038/s41467-023-39046-8.
[34] Li W, Berlinicke C, Huang Y, Giera S, McGrath AG, Fang W, et al. High-throughput screening for myelination promoting compounds using human stem cell-derived oligodendrocyte progenitor cells. iScience 2023 Feb 8;26(3):106156. https://doi.org/10.1016/j.isci.2023.106156.
[35] Wu MY, Wong AYH, Leung JK, Kam C, Wu KL, Chan YS, et al. A near-infrared AIE fluorescent probe for myelin imaging: from sciatic nerve to the optically cleared brain tissue in 3D. Proc Natl Acad Sci U S A 2021 Nov 9;118(45):e2106143118. https://doi.org/10.1073/pnas.2106143118.
[36] Seiler S, Wälti CM, de Barros V, Barbash S, Foo LC. Higher throughput workflow with sensitive, reliable and automatic quantification of myelination in vitro suitable for drug screening. Sci Rep 2023 Feb 18;13(1):2883. https://doi.org/10.1038/s41598-023-29333-1.